High-pressure phase transition and properties of spinel $ZnMn_2O_4$

S. Åsbrink*

Department of Inorganic Chemistry, Arrhenius Laboratory, Stockholm University, 106 91 Stockholm, Sweden

A. Waśkowska

Institute of Low Temperature and Structure Research, Polish Academy of Sciences, 50 950 Wrocław, Poland

L. Gerward

Department of Physics, Technical University of Denmark, 2800 Lyngby, Denmark

J. Staun Olsen

Niels Bohr Institute, Ørsted Laboratory, University of Copenhagen, 2100 Copenhagen, Denmark

E. Talik

Institute of Physics, Silesian University in Katowice, 40 007 Katowice, Poland

(Received 16 June 1999)

X-ray photoelectron spectroscopy, magnetic measurements, and a single-crystal x-ray structure determination at normal pressure have shown that Jahn-Teller active manganese ions in $ZnMn_2O_4$ are present in one valence state (III) on the octahedral sites of the spinel structure. The high-pressure behavior of $ZnMn_2O_4$ was investigated up to 52 GPa using the energy-dispersive x-ray diffraction technique and synchrotron radiation. The structural first-order phase transition from the body-centered to primitive-tetragonal cell takes place at $P_c = 23$ GPa. The high-pressure phase is metastable down to normal pressure. The c/a ratio reduces from 1.62 to 1.10 above P_c and remains nearly pressure independent in the high-pressure phase. The transition is attributed to the changes in electron configuration of the Mn^{3+} ions. According to the crystal field theory, the e_g electron of octahedrally coordinated Mn^{3+} is either in the d_z^2 orbital or in the $d_{x^2-y^2}$. In the first configuration the MnO_6 octahedron will be elongated and this is the case at normal pressure, while the second configuration gives the flattened octahedron. In the high-pressure phase some proportion of the e_g electrons of the Mn^{3+} ions is moved to the $d_{x^2-y^2}$ level, which is revealed as an abrupt fall of observed magnitude of the distortion of the bulk crystal above P_c. [S0163-1829(99)08341-1]

I. INTRODUCTION

Mixed transition-metal oxides with spinel structure have been widely studied from various aspects, giving rise to much discussion, but two important and interrelated points of interest are still a subject of development. One is associated with the magnetic, electronic, and transport phenomena and the other with the elastic properties of the Jahn-Teller active cation system. Early crystal structure and crystal chemistry investigations, reported in the literature, e.g., Refs. 1–8, have shown that the interesting properties of spinels are determined by the cation valence and cation distributions between the tetrahedral (A) and octahedral (B) interstices of the cubic close-packed arrangement of the oxygen sublattice. In terms of crystal field theory, the electrostatic interactions of the ligands strongly affect the electronic configuration of the central metal ion and hence the properties of the material.

The present work is a part of our systematic study of high-pressure effects on the structure of the oxide spinels. We have focused our interest on $ZnMn_2O_4$, which at room temperature shows a normal cation distribution and is tetragonally distorted $c'/a' = 1.14$, where a' and c' refer to the face-centered pseudocubic cell with $a' = 8.087$ Å, $c' = 9.245$ Å and the cell volume V'.[1] The volume V' is twice of that of the body-centered cell $I4_1/amd$.[5] The distortion is

caused by the Jahn-Teller (JT) instability of $Mn^{3+}(d^4)$, located on the B sites of the oxygen sublatice.[9–11] Zn^{2+} with a filled outermost electronic shell d^{10} is not JT active and has a strong preference for the A sites. Between the spins of Mn^{3+} ions, separated by the oxygen anions, various magnetic interactions have been suggested and their properties have been a subject of several studies.

However, the reports on $ZnMn_2O_4$ are rather confusing. Some authors[12] have claimed a Néel temperature at about 200 K, which is unusually high for a collinear spin array of the Mn^{3+} ions at the adjacent octahedral sites. In Ref. 13 a helical spin arrangement has been reported to disappear between 48 and 80 K. A weak change in the slope of the curve showing the temperature dependence of magnetic susceptibility $\chi(T)$ in the interval 4.2–50 K was not conclusive either.[14] Thermal difference analysis[13] (DTA) has shown a phase transition at 230 or 271 K with strong metastability effects, but not related to any structural changes. These authors suggest that metastability phenomena could be the origin of discrepancy in the magnetic behavior. The effect of temperature on the structure of $ZnMn_2O_4$ has been studied by high-temperature powder x-ray diffraction.[15] At 1323 K a first-order phase transition to the cubic form Fd-$3m$ has been observed. The structural model of the transition was based on two concommitant mechanisms: the randomiza-

TABLE I. Details of single-crystal x-ray data collection and structure refinement at normal conditions.

Crystal data:	
Crystal system	Tetragonal
Space group	$14_l/amd$
a (Å)	5.720(1)
b (Å)	9.245(2)
V (Å^3)	302.48(3)
Z	4
Density calc. (Mg/m^3)	5.254
Absorption coeff. μ (mm^{-1})	15.91
Data collection:	
Radiation, wavelength (Å)	Mo $K\alpha$, 0.71073
Monochromator	Graphite
2θ range (deg)	96.5
Scan type	$\omega/2\theta$
Scan width (deg)	$1.1+0.25\tan\theta$
Index range	h: -11, 0
	k: -11, 11
	l: 0, 19
No. reflections collected	3143
No. independent reflections	411
No. observed reflections	327
Decay of standard reflections	Negligible
Refinement:	
Refinement on	F^2
F_o criterium	$|F_o|\geqslant 2\sigma(F_o)$
Corrections:	
Lorentz ploarization	
Absorption (empirical),	
$T_{\min}$ and $T_{\max}$	0.20 and 0.56
Extinction (empirical as in SHELXL93)	$x=0.017(1)$,
R_{int} (before; after absorption)	0.044; 0.0286
Number of varied parameters	10
Final R_1	0.024
Final wR_2	0.050
Goodness of fit	1.003
Min. and max. residual (e Å^{-3})	-1.5,1.7

tion of directions of the individual distorted octahedra at high temperature and the change of concentration of the distorting Mn^{3+} ions at the B sites by the formation of Mn^{2+} and Mn^{4+} ions.

The present high-pressure experiment was performed with an intention to form the cubic phase of $ZnMn_2O_4$. We expected that by applying pressure we would force a change to mixed-valence state of manganese ions. This should result in reducing the amount of JT distorting Mn^{3+} at the B sites, and at some critical concentration of Mn^{3+}, the crystal would adopt the cubic symmetry. Recent studies on another manganese, $NiMn_2O_4$, have disclosed that depending on temperature and pressure conditions, the same cations may show different JT distorting properties related to their electronic state. These differences in the electronic structure are a reason for the appearance of different polymorphic forms of the
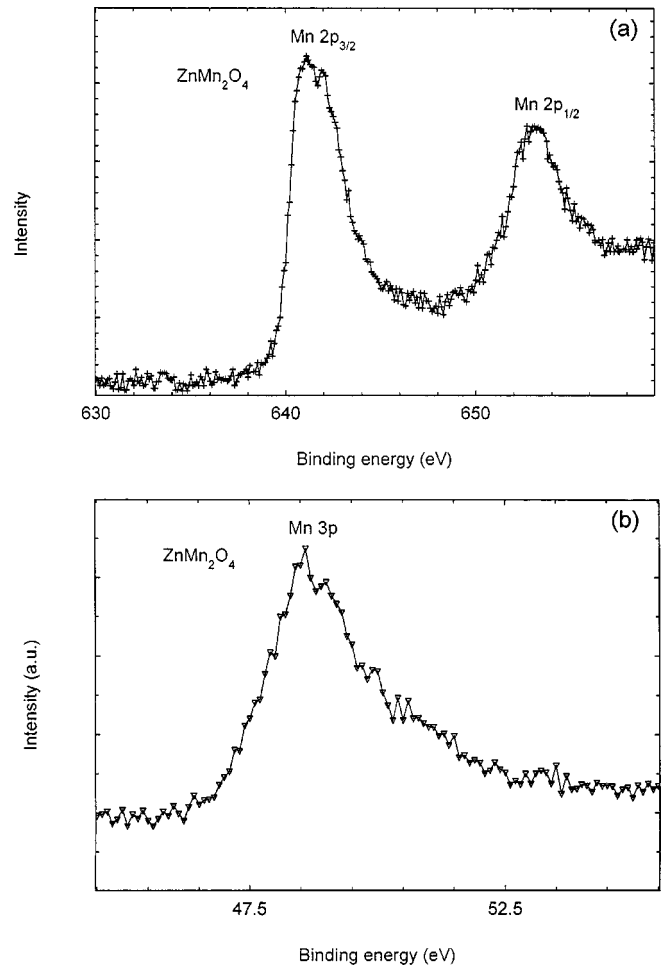
FIG. 1. Mn $2p$ and $3p$ spectra of $ZnMn_2O_4$ at room temperature.

spinel structure. A low-temperature synthesis (473 K) gave the tetragonal structure with $c/a>1$,[16] while in a high-temperature synthesis the cubic form has been obtained.[17] A high pressure, acting on the cubic phase, caused the tetragonal distortion.[18] Therefore, before performing the high-pressure diffraction studies on $ZnMn_2O_4$, we have prepared a well-characterized sample by investigating valence state of
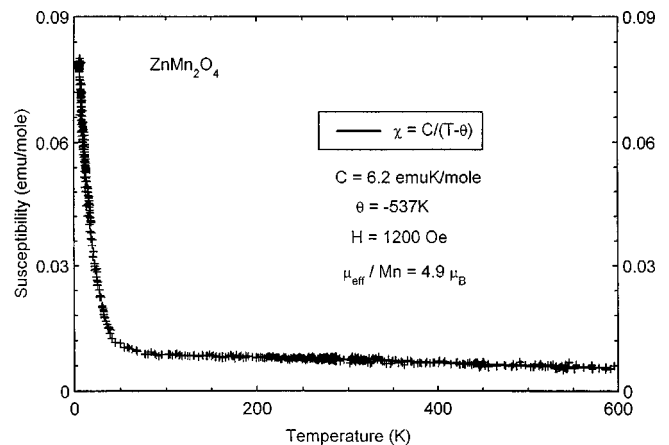

FIG. 2. Temperature dependence of the magnetic susceptibility $\chi(T)$ in an external field of 1200 Oe.

TABLE II. Atomic positional parameters and thermal displacement amplitudes U_{iso} (Å^2).

Atom	Site	x	y	z	U_{iso}
Zn	$4(a)$	0	0.75	0.125	0.0102(2)
Mn	$8(d)$	0	0.5	0.5	0.0118(3)
O	$16(h)$	0	0.0250(2)	0.2556(2)	0.0144(6)

the metal ions, the magnetic properties, and the x-ray single-crystal structure.

II. EXPERIMENT

The single crystals were grown from stoichiometric amounts of ZnO and MnO_2 sintered at 1173 K in evacuated silica tube. After 5 days the tube was quenched. The composition was analyzed by x-ray diffraction in a Guinier camera. X-ray photoelectron spectroscopy (XPS) measurements were carried out with PHI 5700/660, a Physical Electronics spectrometer, to investigate the cation valence using monochromated Al $K\alpha$ radiation. The spectra of photoelectrons as a function of their kinetic energy were analyzed by a hemispherical mirror analyzer with an energy resolution of about 0.3 eV. The samples were broken under high-vacuum conditions, in the low 10^{-10} Torr range, to obtain a fresh surface. The carbon C $1s$ binding energy (284.7 eV) was used for calibration. The electron-microscopic observations confirmed a good quality of the single crystal. The magnetic susceptibility was measured using a Faraday magnetometer in an external fields of 1200 Oe over a temperature interval 4.2–600 K. Single-crystal x-ray diffraction data for structure determination at normal conditions were measured with a Kuma KM-4 diffractometer, using the conditions given in Table I. Thirty-eight reflections with $7° < \theta < 18°$ were used in the least-squares calculation of the unit cell constants and which hereafter refer to the $I4_1/amd$ space group. The crystal stability and orientation were monitored by periodically checking the intensities of three standard reflections. The raw intensities were corrected for Lorentz-polarization effects and the absorption was evaluated with the ψ scan scheme,
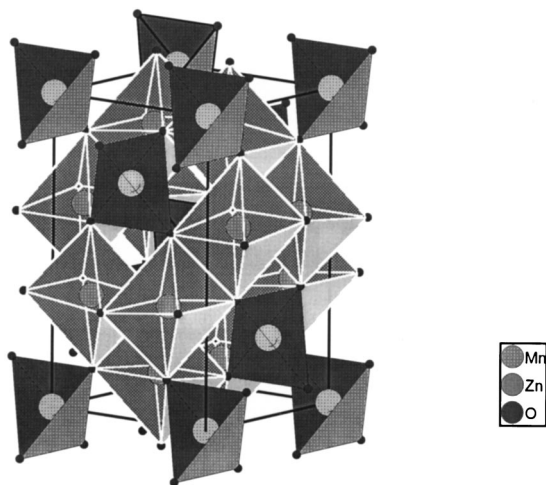

FIG. 3. Crystal structure of $ZnMn_2O_4$. The origin of the unit cell is at the center ($2/m$) of the space group $I4_1/amd$.

TABLE III. Selected bond and interatomic distances (in Å) and bond angles (in degrees).

	Distances (Å)		Angles (deg)	
Zn-O	1.983(1)	4×	O-Zn-O	111.77(5)	4×
Mn-O	1.925(1)	4×	O-Zn-O	104.96(9)	2×
Mn-O	2.264(1)	2×	O-Mn-O	180(0)	3×
Mn-Mn$_{-x,1/2-y,z}$	2.860(0)	2×	O-Mn-O	83.94(6)	2×
Mn-Mn$_{1/4-x,3/4+x,1/4+z}$	3.071(1)	4×	O-Mn-O	85.76(6)	4×
			O-Mn-O	94.24(6)	4×
			O-Mn-O	96.06(6)	2×

using the procedure given in the structure solution program system SHELXL'90. High pressures in the range 0–58 GPa were obtained in a Syassen-Holzapfel-type diamond-anvil cell. The sample and the ruby chip were inserted in a hole of diameter 0.2 mm in an Inconel gasket. A mixture of methanol and ethanol (4:1) was used as the pressure transmitting medium. The pressure was determined by the wavelength shift of the ruby red line using the nonlinear pressure scale.[19] The Bragg angle was calculated from a zero-pressure diffraction spectrum of NaCl in the diamond-anvil cell. The x-ray powder diffraction spectra have been obtained using synchrotron radiation and the white-beam energy dispersive method at the Hamburg Synchrotron Radiation Laboratory, HASYLAB, Hamburg, Germany.
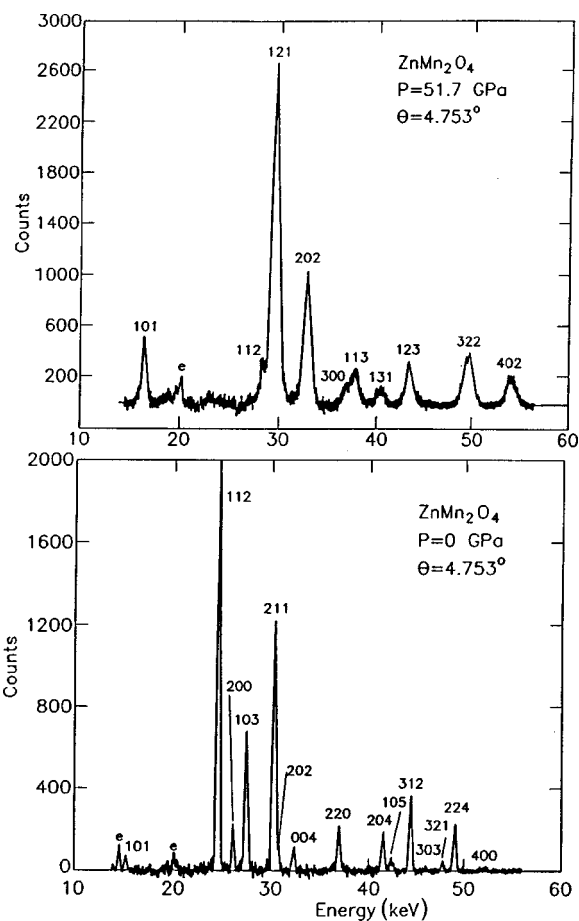

FIG. 4. Synchrotron x-ray powder diffraction data taken at $P \approx 0$ and 51.7 GPa, respectively.
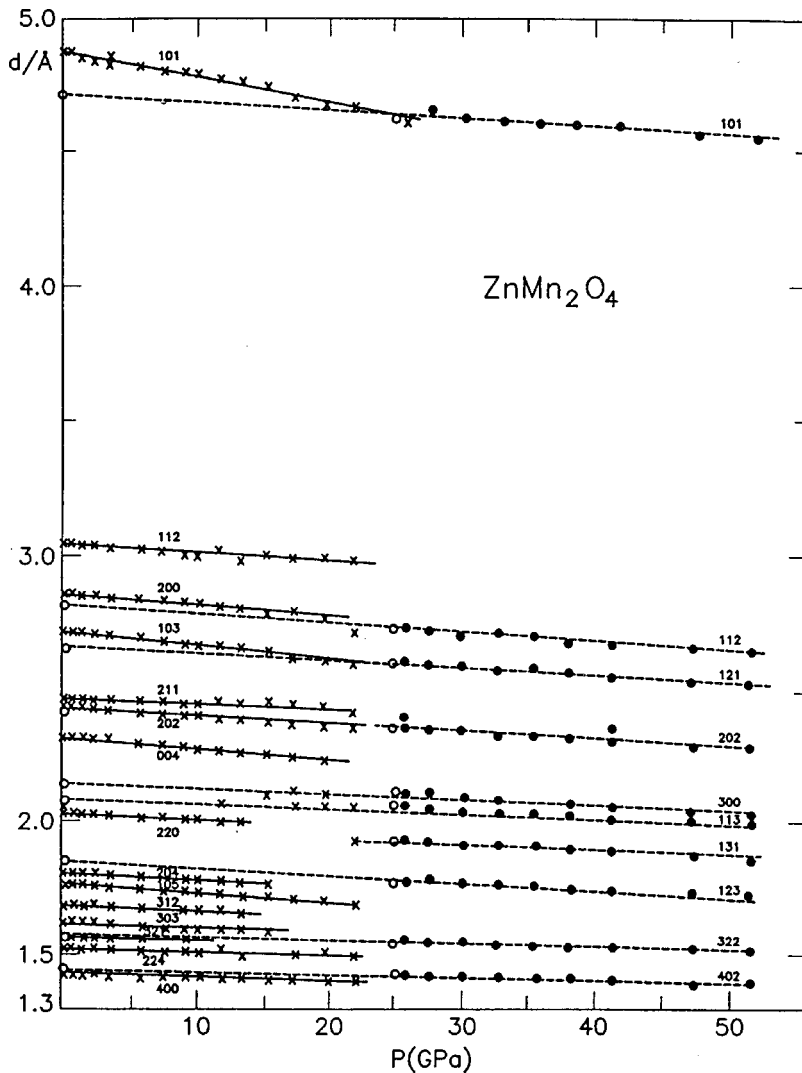
FIG. 5. Pressure change of the interplanar spacings. The corresponding critical pressure is 23(1) GPa.

III. RESULTS AND DISCUSSION

The spectroscopy of electron core levels gives direct information on the valence of $3d$ cations. XPS spectra corresponding to the binding energies of the Mn core levels $2p$ and $3p$ are shown in Figs. 1(a) and 1(b), respectively. The Mn $2p$ spectrum displays a $2p_{3/2}$ and $2p_{1/2}$ spin-orbit doublet at 641.2 and 652.7 eV. The separation of the two signals is 11.5 eV. A detailed analysis of shape of the Mn $2p_{3/2}$ sublevel suggests that the splitting of the signal may be connected with the superexchange process between the Mn^{3+} ions on the octahedral sites. A similar effect was recently reported in Heusler alloys.[20] The narrow signals with full width at half maximum (FWHM) of about 2–2.5 eV are characteristic of manganese ions in one only oxidation state.[21,22] There is no indication of divalent and tetravalent manganese ions.

The temperature dependence of the magnetic susceptibility $\chi(T)$ is shown in Fig. 2. From the stright-line approximation consistent with the Curie-Weiss law at the high-temperature range, the values of the Curie constant C and the paramagnetic Curie temperature θ were obtained. The negative value of θ points to antiferromagnetic interactions below the Néel temperature $T_N = 21.5$ K. The effective magnetic moment $\mu_{\rm eff} = 4.9\mu_B$/Mn evaluated from the experimental data is in good agreement with the magnetic moment based

on a spin contribution of Mn^{3+} with four unpared spins in the high-spin configuration $\mu_s = \sqrt{n(n+2)} = 4.9$ (see, e.g., Ref. 23). This μ value is consistent with a collinear rather than helical spin ordering, as was earlier suggested.[13] The x-ray single-crystal structure at room temperature is isostructural with hausmannite, Mn_3O_4.[24] Atomic positional and thermal displacement parameters are given in Table II. The structure with the tetrahedral and octahedral voids of the oxygen sublattice, centered by Zn^{2+} and Mn^{3+}, respectively, is shown in Fig. 3. It should be noted that a distortion of the structure is revealed mainly on the B sites. The MnO_6 octahedra are elongated with four short [1.925(1) Å] and two long [2.264(1) Å] Mn-O distances (Table III). Such a distortion is typical of Mn^{3+} acting as a JT ion operating on the octahedral site (see, e.g., Refs. 25 and 26). The tetrahedral environment of Zn^{2+} is more symmetric with four identical Zn-O distances, and only the bond angles deviate from the 109.47° value found in the regular tetrahedron. In order to check the site occupation, in one of the refinement models a partial occupation of the metal positions has been assumed in proportions 90%:10% for Zn/Mn in the A site and for Mn/Zn in the B site. The refinement was not stable, however, and had to be abandoned.

Summarizing the studies described above, it can be stated that the spin ordering takes place below $T_N = 21.5$ K and the sample is free from the mixed-valence states of the manga-
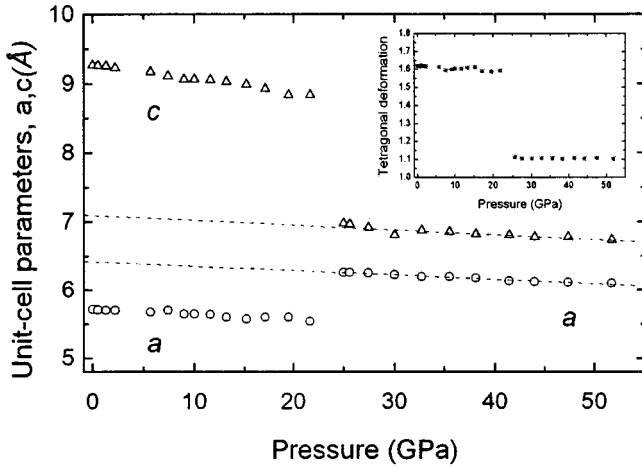
FIG. 6. Unit cell parameters of $ZnMn_2O_4$ as functions of pressure. The inset shows the pressure dependence of the tetragonal deformation c/a.

FIG. 7. Unit cell volume vs pressure.

nese cations; thus, the initial ionic configuration is $Zn^{2+}[Mn^{3+}]_2O_4$. The single-crystal structure of the low-pressure phase with the space group $I4_1/amd$ shows a tetragonal distortion with $c/a=1.62$. The crystals characterized in this way were subsequently used in the high-pressure experiment.

High-pressure diagrams were recorded up to 58 GPa. Two examples are shown in Fig. 4, corresponding to low pressure at ≈ 0 and high pressure at 51.7 GPa, respectively. They differ in a number of peaks, suggesting a phase transition. From the change of interplanar spacings as a function of pressure (Fig. 5) the transition pressure on uploading was $P_c=23$ GPa. Upon decompression the new phase appeared metastable down to normal conditions. The pattern recorded at 51.7 GPa has been indexed according to the primitive tetragonal cell. The pressure dependence of the unit cell constants and the c/a ratio (Fig. 6) exhibit a slightly anisotropic character of the compression, corresponding to the deformation tendency of the MnO_6 octahedra due to the JT effect. The magnitude of the tetragonal distortion has been reduced from 1.62 at ambient pressure to 1.10 above P_c. It is remarkable that the contraction takes place mainly below P_c and there is no substantial compression of the high-pressure phase up to the maximum pressure.

The experimental pressure-volume data (Fig. 7) have been described by Birch equation of state[27] in the pressure range $P<12$ GPa, thus avoiding possible problems with nonhydrostatic pressures above 12 GPa. The equation of state can be written as

$$\frac{P}{B_0}=\frac{3}{2}(x^7-x^5)\left[1+\frac{3}{4}(B_0'-4)(x^2-1)\right], \quad (1)$$

where $x=(V_0/V)^{1/3}$, V is the unit cell volume at pressure P, and V_0 is the zero-pressure volume. B_0 is the bulk modulus and B_0' its pressure derivative, both evaluated at zero pressure. The bulk modulus B_0, obtained from a fit of of Eq. (1) to the data shown in Fig. 7 is 197(5) GPa. The pressure derivative has been constrained to 4.0.
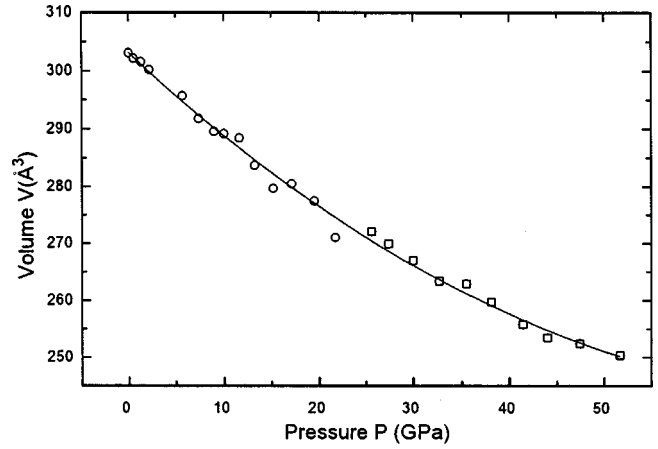
IV. CONCLUSIONS

In $3d$ transition-metal ions, the five d orbitals are split by an octahedral ligand field into a lower triplet t_{2g}, with d_{xy}, d_{yz}, d_{xz} levels, and an upper doublet e_g, with $d_{x^2-y^2}$ and d_{z^2}. Crystal field theory, together with the Jahn-Teller theorem, implies that the symmetric coordination of ligands around the central ion with orbitally degenerate electron configurations of d states is unstable. To remove this degeneracy, the ions distort their coordination polyhedron and, at the same time, stabilize the system. Taking into account the $3d^4$ orbital properties of Mn^{3+} and the octahedral ligand field symmetry, we have initially assumed that the high pressure will increase the orbital degeneracy and the high-spin configuration $t_{2g}\uparrow\uparrow\uparrow e_g\uparrow$ would turn unstable. The system would then tend to stabilize by spin pairing corresponding to the low-spin state $(t_{2g}\uparrow\downarrow\uparrow\uparrow)$. The JT distortion should disappear, and a cubic crystal symmetry should be obtained. It turned out, however, that although the c/a ratio of high pressure has been reduced from 1.62 to 1.10, the new phase remained tetragonal. An explanation of this result could be found if we consider the e_g electron in the high-spin configuration. The JT theory cannot differentiate between the $d_{x^2-y^2}$ and d_{z^2} levels as the most stable in a distorted octahedra
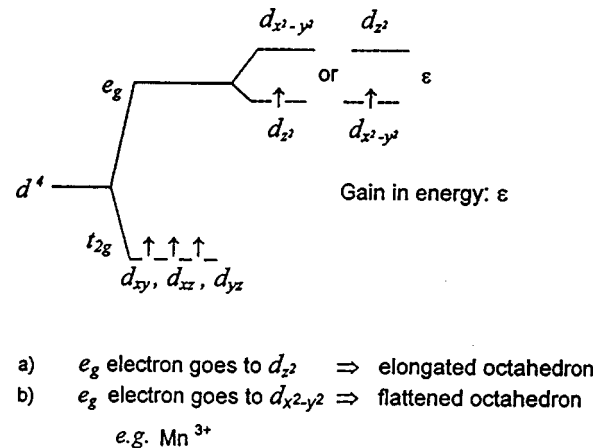

FIG. 8. Two types of Jahn-Teller distortions of the d^4 ions in the octahedral ligand-field: (a) single e_g electron goes to the d_{z^2} shell causing an elongation of the octahedron, and (b) the e_g electron goes to the $d_{x^2-y^2}$, leading to a flattening of the octahedron.

(Fig. 8). Case (a) gives an axially elongated octahedron, and this is, to the best of our knowledge, the only observed distortion in components with Mn^{3+} in an octahedral coordination at normal pressure. Case (b), which theoretically is equally probable, gives a compressed octahedron. The observed tetragonality might be a combination of these two distorting properties of Mn^{3+}. The structural modeling of the high-pressure behavior of tetragonal spinel Mn_3O_4 (ionic configuration $Mn^{2+}[Mn^{3+}]_2O_4$), based on the observed unit cell deformation, showed that axially distorted Mn^{3+} octahedra sites became more regular at the pressure of about 10 GPa.[25] For higher pressures this configuration turned unstable, however, and the subsequent transition led to an orthorhombic phase. Unlike Mn_3O_4, up to the maximum pressure of about 50 GPa, $ZnMn_2O_4$ remains tetragonal. The compressibility of the unit cell above P_c is almost pressure independent. Since c/a is close to unity, it can be inferred that in the bulk crystal the octahedral sites are occupied by the Mn^{3+} cations forming six nearly equivalent bonds. It is therefore likely that the high-pressure structure consists of two types of individually distorted octahedra: one with the e_g electron on the d_{z^2} level (the elongated octahedra) and another type with e_g on the $d_{x^2-y^2}$ levels (the flattened octahedra). At a pressure of about 50 GPa the concentration of the first type Mn^{3+} ions is still dominating. The strongly first-order character of the transition indicates an electronic origin of the pressure effect on $ZnMn_2O$.

---

*Deceased.

[1] F. C. Romeijn, Philips Res. Rep. **8**, 304 (1953).

[2] E. W. Gorter, Philips Res. Rep. **9**, 295 (1954).

[3] J. B. Goodenough and A. L. Loeb, Phys. Rev. **98**, 391 (1955).

[4] A. P. B. Sinha, N. R. Sanjana, and A. B. Biswas, J. Phys. Chem. **62**, 291 (1958).

[5] F. K. Baltzer and J. G. White, J. Appl. Phys. **29**, 445 (1958).

[6] K. S. Irani, A. P. B. Sinha, and A. B. Biswas, J. Phys. Chem. Solids **17**, 101 (1960).

[7] S. Haffner, Schweiz. Mineral. Petrogr. Mitt. **40**, 207 (1960).

[8] G. Blasse, Philips Res. Rep. **3**, 1 (1964).

[9] J. D. Dunitz and L. E. Orgel, J. Phys. Chem. Solids **3**, 20 (1957).

[10] L. E. Orgel, *Introduction to Transition-Metal Chemistry: Ligand-Field Theory* (Methuen, London, 1960).

[11] C. J. Ballhausen, *Introduction to Ligand Field Theory* (McGraw Hill, New York, 1962).

[12] Y. Aiyama, J. Phys. Soc. Jpn. **21**, 1684 (1966).

[13] K. Chhor, J. F. Bocquet, C. Pommier, and B. Chardon, J. Chem. Thermodyn. **18**, 89 (1986).

[14] I. O. Troyanchuk, H. Szymczak, and N. V. Kasper, Phys. Status Solidi A **157**, 159 (1996).

[15] K. S. Irani, A. P. B. Sinha, and A. B. Biswas, J. Phys. Chem. Solids **23**, 711 (1962).

[16] M. de Vidales, R. M. Rojas, E. Vila, and O. Garcia-Martinez, Mater. Res. Bull. **29**, 1163 (1994).

[17] S. Åsbrink, A. Waśkowska, M. Drozd, and E. Talik, J. Phys. Chem. Solids **58**, 725 (1997).

[18] S. Åsbrink, A. Waśkowska, J. Staun Olsen, and L. Gerward, Phys. Rev. B **57**, 4972 (1998).

[19] H. K. Mao, P. M. Bell, J. W. Shaner, and D. J. Steinberg, J. Appl. Phys. **49**, 3276 (1978).

[20] Yu. M. Yarmoshenko, M. I. Katsnelson, E. I. Shreder, E. Z. Kurmaev, A. Ślebarski, S. Plogmann, T. Schlathölter, J. Braun, and M. Neumann, Eur. Phys. J. B **2**, 1 (1998).

[21] V. A. M. Brabers, F. M. van Setten, and S. A. Knapen, J. Solid State Chem. **49**, 93 (1983).

[22] J. Töpfer, A. Feltz, D. Gräf, B. Hackl, L. Raupach, and P. Weissbrodt, Phys. Status Solidi A **134**, 405 (1992).

[23] D. J. Khomsky and G. A. Sawatzky, Solid State Commun. **102**, 87 (1997).

[24] P. Chardon and F. Vigneron, J. Magn. Magn. Mater. **58**, 128 (1986).

[25] C. R. Ross II, D. C. Rubie, and E. Paris, Am. Mineral. **75**, 1249 (1990).

[26] H. Yamaguchi, A. Yamada, and H. Uwe, Phys. Rev. B **58**, 8 (1998).

[27] F. Birch, J. Appl. Phys. **9**, 279 (1938).